

Near-field measurements of a single-mode optical fiber and $\text{Er}^{3+}:\text{Ti}:\text{LiNbO}_3$ and $\text{Ti}:\text{LiNbO}_3$ optical waveguides

G. C. VASILE*, N. N. PUȘCAȘ^a

University "Politehnica" Bucharest, Physics Department, Splaiul Independentei, 313, 060042, Bucharest, Romania

^a*University "Politehnica" Bucharest, Physics Department, Splaiul Independentei, 313, 060042, Bucharest, Romania*

In this paper we report some experimental results concerning the near-field measurements of optical fibers and $\text{Er}^{3+}:\text{Ti}:\text{LiNbO}_3$ and $\text{Ti}:\text{LiNbO}_3$ optical waveguides for a laser radiation having 1540 nm wavelength. These near-field measurements have been performed using an infrared vidicon camera with various functions for image processing, good resolution and stability. The objective of this paper is to evaluate some basic parameters, like: number of modes, dimensions of mode, the simetrie, penetration depth and the refractive-index profile which characterize the optical fibers and waveguides. These parameters are important from the point of view of their applications in telecommunication and sensing.

(Received May 16, 2011; accepted June 9, 2011)

Keywords: Single-mode optical fiber, $\text{Er}^{3+}:\text{Ti}:\text{LiNbO}_3$ and $\text{Ti}:\text{LiNbO}_3$ optical waveguides, Near-field measurements, Mode profile, Infrared vidicon camera

1. Introduction

The optical fiber is an optical waveguide which circular section and consists of a cylindrical central dielectric core clad by a material of slightly lower refractive index. In present, the optical fibers plays a very important role in the telecommunication and sensing fields being used in diverse applications.

The lithium niobate substrate is widely used in a variety of integrated devices due to its unique electro-optical, photoelastic, piezoelectric and non-linear properties. Thus, the passive and active (doped with Nd^{3+} , Er^{3+} , Yb^{3+} etc. ions) optical waveguides based on lithium niobate substrate have attracted great interest in the field of integrated optics. Erbium-doped integrated waveguides are attracting and due to their 1,5 μm operation band and their application to optical communication as integrated optical amplifiers or lasers. To estimate the performance of any active waveguide device is very important to knowledge the characteristics of the waveguides such as the mode profile, the refraction index profile, the losses, emission and absorption cross sections for active waveguides. All this are the principal characteristics of optical waveguides.

From near-field measurements we have obtained the mode profile which is an important characteristic of optical fibers and waveguides [1] – [8]. From de mode profile we have obtained the informations regarding the number of modes, dimensions of mode, the simetrie, penetration depth and the refractive-index profile.

The structure of the paper is the following: in Sect. 2 we present the basic theory of near-field measurement, the

relations used for the determination of the refractive-index profile and in Sect. 3 we report the experimental setup and discuss the obtained results. The conclusions of the paper are outlined in Sect. 4.

2. Theoretical considerations

Theoretical the near-field method is based on solving the scalar wave equation for refractive index profile, knowing the transversal electric field distribution of the waveguide's mode. The normalized electric field profile can be calculated from the intensity profile of the fundamental mode $I(x, y)$:

$$\psi(x, y) = \sqrt{\frac{I(x, y)}{I_{\max}}}, \quad (1)$$

where x and y are the coordinates of the transverse section of the waveguide and I_{\max} is the maximum value of the intensity. In the scalar approximation the field is transversal and completely described by the linearly polarized mode, solution of the Helmholtz scalar equation [1], [7]:

$$\Delta_T \psi(x, y) + [k_0 n^2(x, y) - \beta^2] \psi(x, y) = 0 \quad (2)$$

where Δ_T is the traverse Laplace operator, $\psi(x, y)$ represents the transverse electric or magnetic field, $n(x, y)$ is the refractive-index profile, $\beta = kN_{\text{eff}}$ is the

propagation constant, N_{eff} is the effective index and $k_0 = 2\pi/\lambda$ is the wave number of the vacuum. The effective index is not known exactly, but it is approximately equal to the substrate index value. The refractive-index profile may be determined from Eq. (2) as:

$$n^2(x, y) = \left(\frac{\beta}{k_0}\right)^2 - \frac{1}{k_0^2} \frac{\Delta_T \psi(x, y)}{\psi(x, y)}. \quad (3)$$

Making the substitution for intensity $I(x, y) = \psi^2(x, y)$ and introducing:

$$n(x, y) = \Delta n(x, y) + n_s, \quad (4)$$

where n_s is the index substratum one obtained:

$$\Delta n(x, y) \approx \left(\frac{\beta}{k_0}\right) - \frac{1}{2n_s k_0^2 \sqrt{I(x, y)}} \cdot \left(\frac{d^2 \sqrt{I(x, y)}}{dx^2} + \frac{d^2 \sqrt{I(x, y)}}{dy^2}\right) - n_s. \quad (5)$$

The second derivative of the intensity profile at the data point i is numerically calculated following:

$$\begin{aligned} & \frac{1}{\sqrt{I(x, y)}} \left(\frac{d^2 \sqrt{I(x, y)}}{dx^2} + \frac{d^2 \sqrt{I(x, y)}}{dy^2}\right) = \\ & = \frac{\sqrt{I_{i-1,j}} + \sqrt{I_{i+1,j}} - 2\sqrt{I_{i,j}}}{\Delta x^2 \sqrt{I_{i,j}}} + \\ & + \frac{\sqrt{I_{i,j-1}} + \sqrt{I_{i,j+1}} - 2\sqrt{I_{i,j}}}{\Delta y^2 \sqrt{I_{i,j}}} \end{aligned}, \quad (6)$$

where $\sqrt{I(x, y)} = \sqrt{I_{i,j}}$, and Δx , Δy are the horizontal and vertical spacing between data points.

The most important advantages of refractive-index profile reconstruction from the near field measurement method are: the measurement method is direct, non-destructive and the single-mode waveguide is characterized at the operating wavelength. The major disadvantage is that the near field measurements are affected by many sources of errors, such as noise, errors due to the detection system, non-ideal focusing, etc. This imposes the necessity to filter the experimental data of the near field measurements before to use them to determine the refractive-index profile.

3. Experimental set-up and results

Experimental the near-field technique is based on the measurement of the intensity profile of the light transmitted from a waveguide. The near-field intensity

profile of the Er³⁺:Ti:LiNbO₃ and Ti:LiNbO₃ optical waveguides has been measured using the experimental set-up shown in Fig. 1. The laser source at $\lambda = 1540$ nm is coupled into a single-mode optical fiber. For fiber-to-waveguide and fiber-to-fiber coupling is necessary a great precision. An important aspect of fiber coupling is the fiber termination. Without a clean fiber cleave it is practically impossible to couple light into optical fiber.

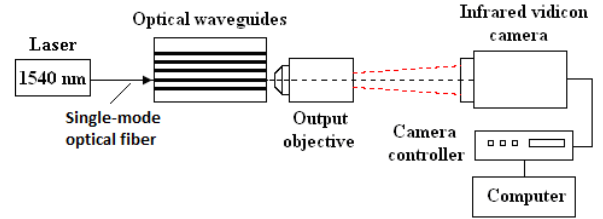


Fig. 1. Experimental set-up for near-field measurements.

The mode profile at output of the optical waveguide is magnified through a 20x microscope objective (with numerical aperture $N.A. = 0.4$) and acquired using a Hamamatsu Infrared Vidicon camera. Because we used this type of camera for to acquire the fundamental mode image we must correct the measured intensity. Thus, the field intensity $I(x, y)$ is calculated from the measured intensity $I'(x, y)$ and the nonlinearity coefficient γ of the vidicon camera using the relation:

$$I(x, y) = I'(x, y)^{\frac{1}{\gamma}}. \quad (7)$$

The value of the nonlinearity coefficient is 0.6 for the device used in our work.



Fig. 2 a), b). Near-field image of the fundamental mode in a Er³⁺:Ti:LiNbO₃ Waveguide a) and single - mode optical fiber b).

The dimension of the acquired image depends on the objective magnification and the distance between the objective and the infrared vidicon camera. Taking into account by the distance between the microscope objective and camera the conversion factor $pixel/\mu m$ has been determined by calibration with a reference object, a small ruler etched into a silica glass with pitch $2 \mu m$. The data acquisition has been performed with a program developed using the language LabView 7.0 from National Instruments.

In Figs. 2. a) and b) we present the near-field image of the fundamental mode in a X-cut $\text{Er}^{3+}:\text{Ti}:\text{LiNbO}_3$ waveguide with a $5\ \mu\text{m}$ width and $54\ \text{mm}$ length and in a single-mode optical fiber, respectively.

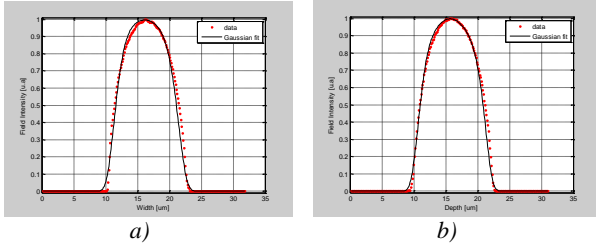


Fig. 3 a, b). Lateral (a) and in-depth (b) mode profiles of measured near-field intensity and fitted curve with a Gaussian function for a single-mode optical fiber.

Up to 10 intensity profiles has been measured for any optical fiber and waveguide and here we presented the average profile obtained. The intensity mode profile of a single-mode optical fiber, whose parameters were $n_{\text{core}} = 1.468$, core diameter $8.2\ \mu\text{m}$, $\lambda = 1.55\ \mu\text{m}$ and mode-field diameter $10.4 \pm 0.5\ \mu\text{m}$, are presented in Fig. 3. For this single-mode optical fiber we obtained the $10.185 \pm 0.043\ \mu\text{m}$ mode field diameter at $\lambda = 1.54\ \mu\text{m}$. These values have been calculated at $1/2$ from intensity. It can be seen that the value obtained is in good agreement with the technical data of the fiber. So, the obtained result encouraged us to apply the method to experimental field profiles of optical waveguides.

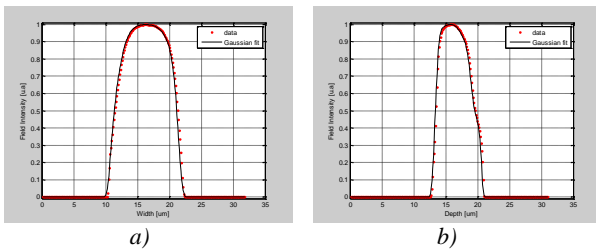


Fig. 4 a), b). Lateral (a) and in-depth (b) mode profiles of measured near-field intensity and fitted curve with a Gaussian function for an $5\ \mu\text{m}$ width and $50\ \text{mm}$ length X-cut $\text{Ti}:\text{LiNbO}_3$ optical waveguide.

In Figs. 4 a), b) and 5 a), b), respectively we present the intensity mode profile for X-cut $\text{Er}^{3+}:\text{Ti}:\text{LiNbO}_3$ and $\text{Ti}:\text{LiNbO}_3$ optical waveguides. For an $5\ \mu\text{m}$ width and $50\ \text{mm}$ length X-cut $\text{Ti}:\text{LiNbO}_3$ optical waveguide we obtained the $9.79\ \mu\text{m}$ width and $6.14\ \mu\text{m}$ depth of the fundamental mode. The corresponding penetration depths, calculated at $1/e$ from intensity, are: $10.48\ \mu\text{m}$ in width and $6.93\ \mu\text{m}$ in depth. For an $5\ \mu\text{m}$ width and $54\ \text{mm}$ length X-cut $\text{Er}^{3+}:\text{Ti}:\text{LiNbO}_3$ optical waveguide we obtained the $7.62\ \mu\text{m}$ width and $4.91\ \mu\text{m}$ depth of the fundamental mode. In this case the corresponding penetration depths are: $8.85\ \mu\text{m}$ in width and $5.49\ \mu\text{m}$ in

depth. We obtained a symmetrical profile in width and asymmetrical profile in depth of the fundamental mode. Looking the Figs. 4 and 5 is important to notice the difference between the mode sizes measured in an Er^{3+} -doped waveguide compared with those measured in a non-doped waveguide. The optical waveguides non-doped confine well the light at $1540\ \text{nm}$ wavelength. In contrast with these in the Er^{3+} -doped optical waveguides the mode has been attenuated. This attenuation is due to absorption by Er^{3+} ions within the optical mode volume.

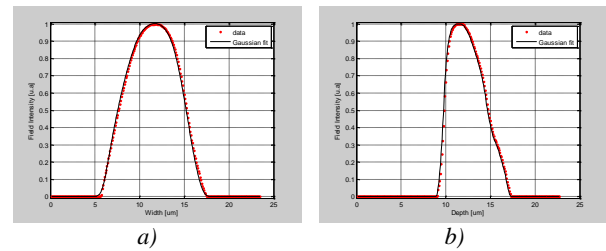


Fig. 5 a), b). Lateral (a) and in-depth (b) mode profiles of measured near-field intensity and fitted curve with a Gaussian function for an $5\ \mu\text{m}$ width and $54\ \text{mm}$ length X-cut $\text{Er}^{3+}:\text{Ti}:\text{LiNbO}_3$ optical waveguide.

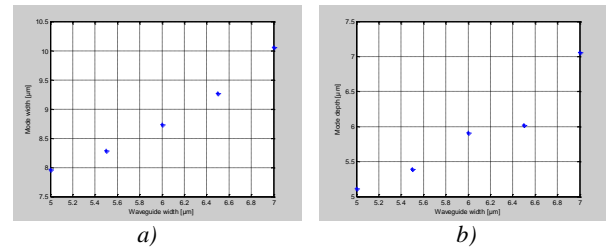


Fig. 6 a), b). a) Width and b) depth of mode versus width of optical waveguide for $54\ \text{mm}$ length X-cut $\text{Er}^{3+}:\text{Ti}:\text{LiNbO}_3$ optical waveguides.

In Fig. 6 a), b), respectively we present the width and depth of mode versus width of optical waveguide for the $54\ \text{mm}$ length X-cut $\text{Er}^{3+}:\text{Ti}:\text{LiNbO}_3$ optical waveguides. The mode sizes increase with the increase of width of the optical waveguides.

For the reconstruction of the refractive index profile only the fundamental mode has been excited. Taking into account of the theoretical considerations presented we reconstructed the refractive-index profile from the near-field intensity profiles. For $\text{Er}^{3+}:\text{Ti}:\text{LiNbO}_3$ and $\text{Ti}:\text{LiNbO}_3$ optical waveguides the values of horizontal and vertical spacing between data points have been $\Delta x = 0.085\ \mu\text{m}$ and $\Delta y = 0.083\ \mu\text{m}$, respectively $\Delta x = 0.116\ \mu\text{m}$ and $\Delta y = 0.113\ \mu\text{m}$. In Figs. 7 a), b) and 8 a), b) we showed the refractive index profile for the X-cut $\text{Ti}:\text{LiNbO}_3$ and $\text{Er}^{3+}:\text{Ti}:\text{LiNbO}_3$ optical waveguides and in Fig. 9 we showed the refractive index profile for the single-mode optical fiber.

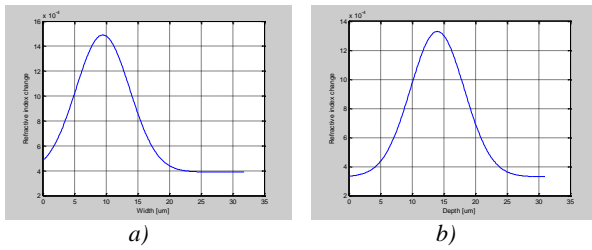


Fig. 7 a), b). Lateral (a) and in-depth (b) refractive index profile for an $5 \mu\text{m}$ width and 50 mm length X-cut $\text{Ti}:\text{LiNbO}_3$ optical waveguide.

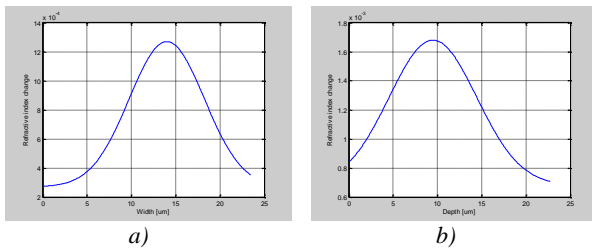


Fig. 8 a), b). Lateral (a) and in-depth (b) refractive index profile for an $5 \mu\text{m}$ width and 54 mm length X-cut $\text{Er}^{3+}:\text{Ti}:\text{LiNbO}_3$ optical waveguide.

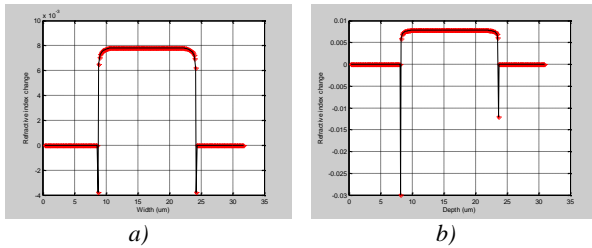


Fig. 9 a), b). Lateral (a) and in-depth (b) refractive index profile for a single-mode optical fiber.

From the refractive index profiles in the case of $\text{Ti}:\text{LiNbO}_3$ optical waveguide (Fig. 7) we obtained for the width refractive index difference the value $\Delta n = 1.489 \cdot 10^{-3}$ while in depth the corresponding value is $\Delta n = 1.329 \cdot 10^{-3}$. Also, we obtained for the width refractive index difference the value $\Delta n = 1.275 \cdot 10^{-3}$ and for the depth refractive index difference the value $\Delta n = 1.683 \cdot 10^{-3}$ for the $\text{Er}^{3+}:\text{Ti}:\text{LiNbO}_3$ optical waveguide (Fig. 8). For the single-mode optical fiber the recovered parameters are: $\Delta n_x = 7.827 \cdot 10^{-3}$ and $\Delta n_y = 7.825 \cdot 10^{-3}$ (Fig. 9).

4. Conclusions

Based on near-field measurements using an infrared vidicon camera we evaluated several parameters: the number of modes, dimensions of modes, the simetrie of the guide, the penetration depths and the refractive-index profile in the case of $\text{Er}^{3+}:\text{Ti}:\text{LiNbO}_3$ and $\text{Ti}:\text{LiNbO}_3$ optical waveguides and single-mode optical fiber, respectively for a laser radiation having 1540 nm wavelength.

The obtained results are in good agreement with others obtained with other methods [1], [2], [7], and may be used for the design and improvement of the complex optoelectronic integrated components.

Acknowledgments

This paper is supported by the Sectoral Operational Programme Human Resources Development, financed from the European Social Fund and by the Romanian Government under the contract number POSDRU/89/1.5/S/64109.

References

- [1] Jochen Helms, Joachim Schmidtchen, Bernd Schuppert, Klaus Petermann, IEEE Journal of Lightwave Technology, **8**(5), 625 (1990).
- [2] David Brooks, Shlomo Ruschin, IEEE Photonics Technology Letters, **8**(2), 254 (1996).
- [3] I. Mansour, F. Caccavale, IEEE Journal of Lightwave Technology, **14**(3), 423 (1996).
- [4] Mark L. von Bibra, Ann Roberts, IEEE Journal of Lightwave Technology, **15**(9), 1695 (1997).
- [5] Leon McCaughan, Ernest E. Bergmann, IEEE Journal of Lightwave Technology, **LT-1**(1), 241 (1983).
- [6] Katsumi Morishita, IEEE Journal of Lightwave Technology, **LT-4**(8), 1120 (1986).
- [7] N. N. Puscas, D. M. Grobncic, I. M. Popescu, M. Guidi, D. Scarano, G. Perrone, I. Montrosset, Optical Engineering, **35**(5), 1311 (1996).
- [8] Fatadin, I. Ives, D. Wicks, M., Journal of Lightwave Technology, **24**(12), 5067 (2006).

*Corresponding author: constantin_g@physics.pub.ro